



Influence of Epoxy Spray Binder on Infusion and Cure in Liquid Composite Molding Processes

Hendrik Möllers¹ · Carsten Schmidt² · Dieter Meiners³

Received: 18 August 2023 / Accepted: 29 November 2023 / Published online: 22 December 2023
© The Author(s) 2023

Abstract

Binders are known to influence the different steps in liquid composite molding process chains. Most research focuses on powder binder and veils. Spray binders are rarely studied. Therefore, the effect of an epoxy spray binder on the infusion and cure steps of liquid composite molding processes is studied in this paper. Permeability measurements, solubility tests and measurements of glass transition temperature, resin cure time and resin viscosity show a complex interaction between binder and resin depending on the process conditions. The binder mostly increased the permeability of the tested preforms. This effect increases with increasing binder loading. At low fiber volume fractions the binder had a positive effect on preform permeability, most likely by delaying the closure of macro flow channels or textile inhomogeneity. The binder did not dissolve in the resin until temperatures of around 120 °C, while remaining as a separate phase at 22 °C, 40 and 80 °C. This has to be considered when defining the cure profile of the resin, as the binder is expected to participate in the cure reaction. The glass transition temperature remained unchanged for the binder-resin combination used. An increase in viscosity by a factor of 1.5-2 was observed when the binder was dissolved in the resin. Samples with dissolved binder cured slightly faster than pure resin. The experimental results were theoretically transferred to real infusion processes.

Keywords Fiber-reinforced Plastics · Composites · Binder · Infusion · Permeability

✉ Hendrik Möllers
hendrik.moellers@tu-clausthal.de

¹ Institute of Polymer Materials and Plastics Engineering, Clausthal University of Technology, Ottenbecker Damm 12, Stade, Germany

² Institute of Production Engineering and Machine Tools, Leibniz Universität Hannover, Ottenbecker Damm 12, Stade, Germany

³ Institute of Polymer Materials and Plastics Engineering, Clausthal University of Technology, Agricolastr. 6, Clausthal-Zellerfeld, Germany

1 Introduction

Fiber-reinforced composites are widely used in a variety of applications ranging from sports equipment to automotive and aerospace applications due to their generally high stiffness, low density and fatigue and corrosion resistance [1]. In liquid composite molding (LCM) processes, a fiber preform is built from individual layers, formed into its final 3D geometry and later infused with a thermoset resin. The process is schematically shown in Fig. 1 So called binders are applied in between the layers to hold the preform in its given shape [2]. Alternatively sewing or stitching techniques are used [3]. Binders can be divided into two groups: reactive and non-reactive binders. Non-reactive binders, mainly thermoplastics, do not interact with the resin and form a separate phase within the manufactured part, whereas reactive binders dissolve in the resin during infusion and react with the hardener component. Reactive binders are often based on thermoset materials [4]. Binders can be used in many different forms. The most common are powders, veils, hot melts, spray adhesives, binders dissolved in solvent and pre-impregnated fibers [5]. Different LCM-processes are used depending on the dimensions and quantities of the part being produced. The different processes require different binders and application techniques. Binder powders or veils must be melted and only fix the textile layers after solidification while spray adhesives and hot melts do not require additional heating steps [6, 7]. Since the binder is applied early in the LCM process, it affects most steps of the processing chain, ranging from preforming to resin infusion to the properties of the final part. Consequently, the influence of the binder on these steps has been subject of research in many publications, mostly focused on powder binders and veils.

Starting with the properties of the preform, it has been found that the binder increases the peel strength between the textile layers. Dickert [5, 8], Brody and Gillespie [4], Möllers et al. [9], Schmidt et al. [7] and Tanoglu et al. [10, 11] found an increase in peel strength with increasing binder loading as long as open surface area is available. The influence of the binder on the first ply adhesion was studied by Helber et al. with similar results [12]. When the textile surface was already fully coated with binder, additional binder did not increase the peel strength further. Dickert [5], Möllers et al. [9] and Coutandin [13] investigated the flexural stiffness of preforms. A linear increase in maximum flexural stress and modulus with increasing binder loading was found for powder binders. Spray binders, which are not solid at room temperature, show a more complex relationship between binder loading and flexural modulus. Creep and relaxation effects are prevalent and the test speed has a significant effect on the test results [9]. While the peel strength is only increased by intra-layer binder, the flexural properties are also enhanced by inter-layer binder [5].

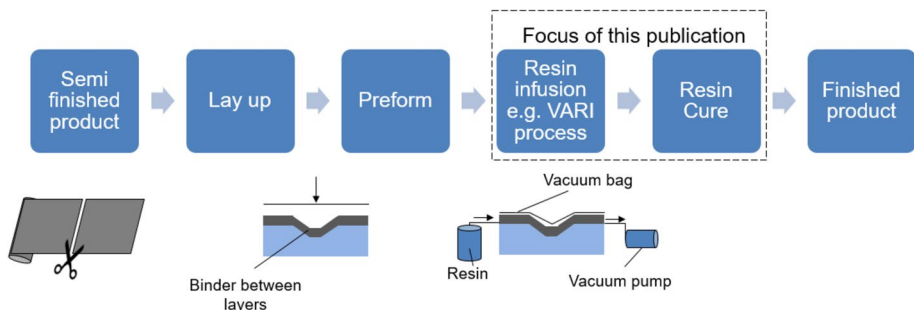


Fig. 1 Steps of liquid composite moulding processes

Several authors have investigated the influence of the binder on the properties of the finished parts. The influence depends mostly on the compatibility of the chosen binder with the resin. The binder can either be incompatible with the resin and remain as a separate phase in the final part, or it can participate in the curing reaction and form a single phase with the resin. As a result, mechanical properties such as fracture toughness, void content, and flexural properties can be affected negatively, positively, or not at all [14–18].

This paper focuses on the influence of the binder on the infusion step, where it can affect the properties of the resin and the permeability of the lay-up. The binder may dissolve in the resin during or after the infusion step, depending on the compatibility of the resin and binder system and the processing temperature. Binders are often made from thermoplastics or thermosets with thermoplastic behavior and a high molecular weight [5]. Therefore, binders can increase resin viscosity and delay the infusion process, especially if the binder is washed out during infusion and higher binder concentrations accumulate at the flow front [2]. Partly contradictory findings have been reported regarding the influence of binder on cure time, glass-transition temperature and total heat release during cure. Brody and Gillespie [15] report an increase in cure time and glass transition temperature and a decrease in total heat released during cure when a thermoplastic binder is mixed into a vinyl ester resin. Lionetto et al. [19] found a decrease in gel temperature and an increase in total heat developed for an epoxy binder dissolved in RTM6 epoxy resin. The influence of the binder on the glass transition temperature of various epoxy resins was investigated by Helber et al. [20], with mixed results depending on the solubility of the binder. This indicates that the particular interaction between the binder and the resin, as well as the properties of the final component, must be taken into account when selecting the binder.

Regarding the influence of the binder on permeability, it is generally expected that binder will decrease permeability for preforms with similar fiber volume fraction, due to the additional volume that is added to the preform, resulting in decreased porosity [2, 21–24]. However, it has also been observed that binders can increase preform permeability, suggesting that they affect preform permeability not only by changing porosity, but also by other means [5, 25, 26]. Dickert [5] describes the resulting permeability as a complex interplay between opposing effects, such as the opening and closing of flow channels or “sealing” of textile surfaces. The combined influence of these effects on permeability can be either positive or negative, depending on the inherent properties of the binder and the processing parameters used (e.g., activation time and temperature). Shih and Lee [26] observed mixed effects on permeability for an epoxy-based powder binder. The permeability decreased when most of the applied binder was present in between the fiber layers. As the activation time and temperature increase, the binder flows off into the fiber tows, causing the tows to shrink and enlarge the flow channels between them. In order to further analyze the effect of the binder, several authors have also calculated the change in preform porosity [2, 5, 27]. Compared to unbindered textiles, the permeability-porosity curve of bindered textiles may resemble the course or deviate significantly depending on the specific textile-binder interactions and varying preforming parameters.

Most of the research presented above focuses on powder binders or veils. They are solid at room temperature and require heat activation in order to fix textile layers in place. Spray binders, on the other hand, are rarely the subject of research. Unlike other types of binders, they are not solid at room temperature, but rather highly viscous. This can result in different behavior during the infusion and curing steps of liquid molding processes. Therefore, additional research is needed on their influence on preform permeability, resin infusion and cure, which is the focus of this paper.

2 Materials and Methods

2.1 Materials

The spray binder used was the epoxy based CeTePox AM1010 from CTP Advanced Materials. The binder can be applied to the textile by swirl spraying using a spray gun or a similar spraying device. At room temperature the binder is highly viscous and does not solidify, providing sufficient tack to bond textile layers together without an additional heating step. The density of the binder is 1.0 g/cm^3 (measured by pycnometer).

The used textile was a carbon fiber non-crimped biaxial fabric by Kümpers with a grammage of 600 g/m^2 fixed with a polyester sewing yarn with a grammage of 6 g/m^2 . The mixed density of the carbon filament and the sewing yarn is 1.89 g/cm^3 (measured by pycnometer). The initial thickness of the textile measured according to DIN EN ISO 5084 is 0.86 mm. For permeability measurements, Wacker AK100 silicone oil was used instead of epoxy resin because of its easier handling. Its viscosity at room temperature is about 100 mPas. The temperature-viscosity relationship of the oil is known and defined in the Matlab script used to evaluate the permeability tests.

HP-E3000RI epoxy resin (Bisphenol A/F) and HP-E30RI amine curing agent (IPD) from HP-textiles were used for solubility tests and to study the influence of the binder on resin curing. The mixing ratio of resin and hardener is 100:30.

2.2 Permeability

2.2.1 Sample Manufacturing

The in-house developed Continuous-Wet-Draping (CWD) process was used to fabricate all bindered samples. It was originally designed to automate the manufacturing of complex curved structures. It has since also been used to manufacture preforms for rotor blades for tidal power plants. Figure 2 shows the CWD lay-up head. The CWD lay-up head is composed of a material storage, a twelve-headed spray module (GHS401-22 SC from Glue-matic) used for binder application, and a pneumatic draping unit. Möllers et al. [9] analyzed the binder spraying and the sample manufacturing in detail. Further information on the CWD lay-up head can be found in Denkena et al. [28] and Bogenschütz et al. [29]. The unbindered samples were cut directly from the fabric.

An overview of all manufactured samples can be found in Table 1. Each sample consists of three $250 \times 250 \text{ mm}$ textile layers sprayed with different binder grammages in between them. Additional samples were made for binder grammages of 0 g/m^2 and 20 g/m^2 to be tested at different fiber volume fractions (V_f). In most applications, binder grammages of 20 g/m^2 or less of CeTePox AM1010 provide sufficient fixation of the preform layers [9]. Therefore, this investigation focused on the differences between samples with binder grammages of 0 g/m^2 and 20 g/m^2 . Additional samples with binder grammages of 40 g/m^2 and 80 g/m^2 were tested at a fiber volume fraction of 50%, as higher binder grammages were predicted to have a greater effect on preform permeability. Three samples were made for each tested combination of binder grammage and fiber volume fraction. The samples were weighted pre testing to calculate the fiber volume fraction together with the sample's edge length and the density of the textile and the binder.

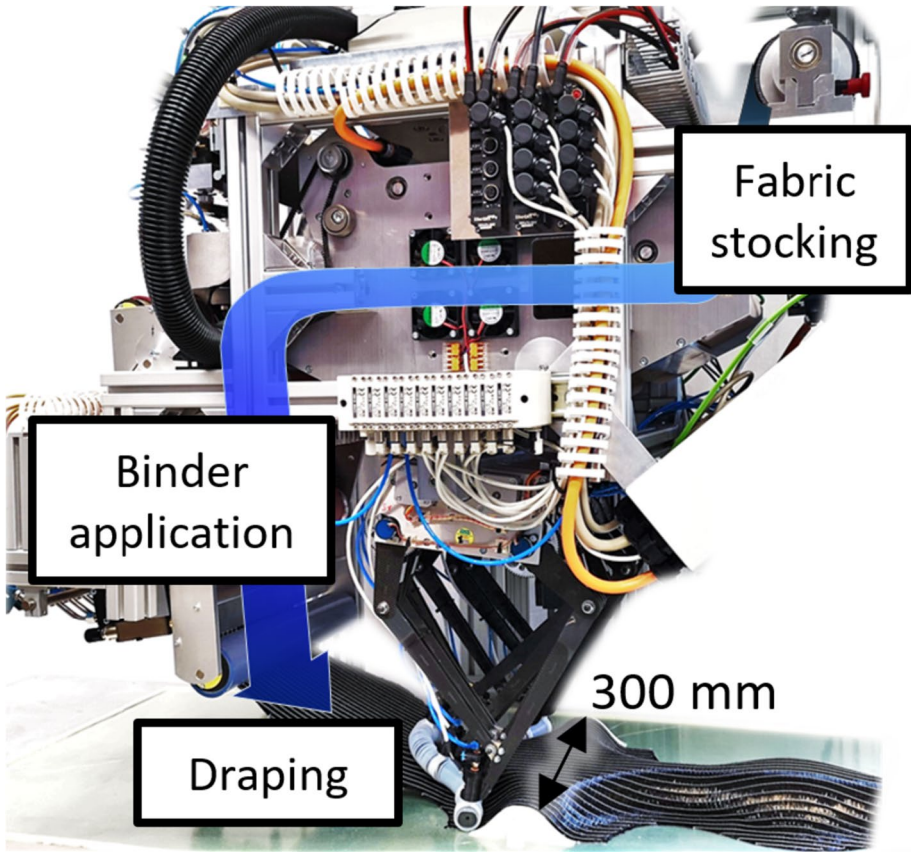


Fig. 2 CWD-Lay-up head

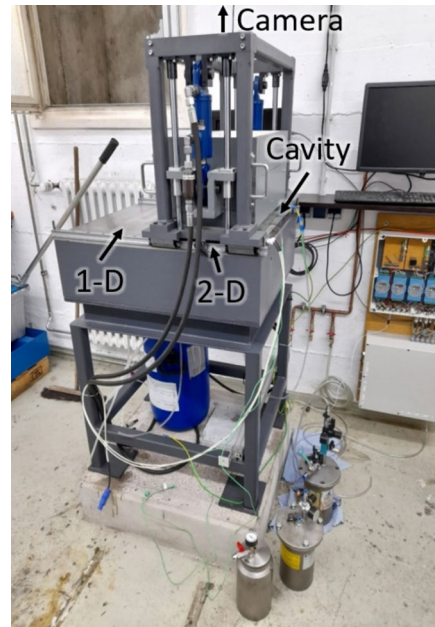
2.2.2 Permeability Measurements

Permeability measurements were carried out on the in-house developed test rig shown in Fig. 3. It was built for 1-D and 2-D permeability measurements using optical flow front tracking but it can also be used for saturated 1-D experiments. Figure 4 shows a schematic drawing of the 2-D test setup used in this paper. The sample is placed on a steel mold and covered with a glass plate. Cavity height is controlled by spacer plates placed next to the sample. Wax pallets are also placed next to the sample to evaluate the uniformity of cavity height after conducting the experiment. After the glass plate is placed on top of the sample, two hydraulic pistons are used to apply 100 bar closing pressure. Sensors are used to measure inlet pressure and temperature. A camera is mounted on top of the test rig to record the flow front at up to 3 fps. Further details regarding the conceptualization, construction and functionality are described by Abliz [30, 31] and Dickert [5]. The recorded data is

Table 1 Sample overview permeability measurements

Binder grammage	0 g/m ²	20 g/m ²	40 g/m ²	80 g/m ²
Sample lay-up	(0/90) ₃	(0/90) ₃	(0/90) ₃	(0/90) ₃

Fig. 3 Permeability test rig for 1-D and 2-D permeability measurements



processed by a Matlab script using difference images to detect the flow front. The local and global permeability for the main axis (K_1) and perpendicular to it (K_2) are calculated using an algorithm described in Fauster et al. [32]. An example of a recorded flow front ellipse and the directions of K_1 and K_2 are shown in Fig. 5. The general functionality of the test rig has been validated by participating in several international benchmark studies [33–36].

Table 2 provides an overview of the cavity heights tested, the resulting fiber volume fractions and the binder grammages used. Silicone oil was used as the test fluid and was injected at a pressure of 1 bar.

Permeability K itself is described by Darcy's law [37] for 1-D linear flow as:

$$K = \frac{v\epsilon\eta}{\nabla P} \quad (1)$$

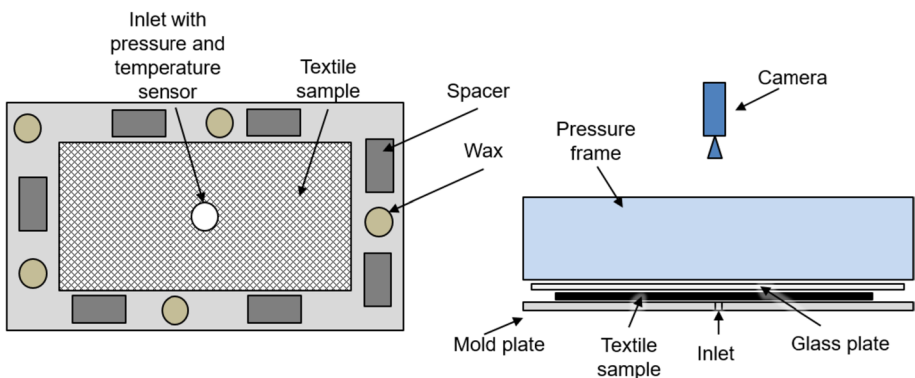


Fig. 4 Schematic drawing of the 2-D test setup (not to scale)

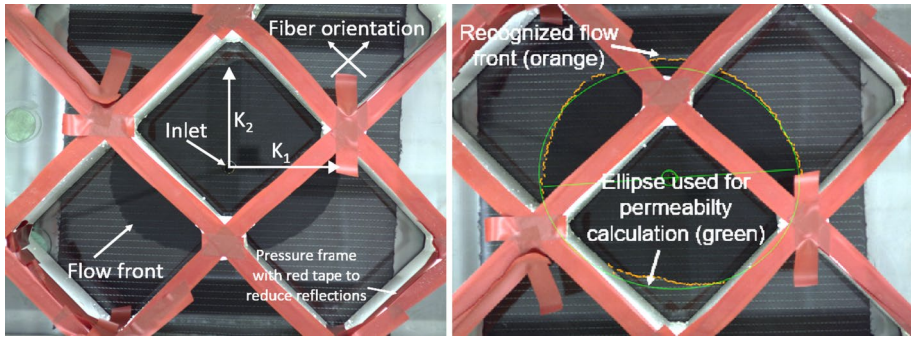


Fig. 5 Example of recorded flow front ellipse and evaluation in Matlab with increased brightness for better flow front visibility (Textile sample 250 mm x 250 mm)

with v : flow velocity, ϵ : porosity, η : dynamic viscosity and ∇P : pressure gradient.

For an anisotropic material like the one used in this publication where an elliptic flow front is expected Darcy’s law can be rewritten as [30]:

$$K_e = \left\{ \bar{r}_f^{-2} \left[2 \ln \left(\frac{\bar{r}_f}{\bar{r}_0} \right) - 1 \right] + \bar{r}_0^{-2} \right\} \frac{1}{t} \frac{\epsilon \eta}{4 \Delta p} \tag{2}$$

with \bar{r} : equivalent radius \sqrt{ab} , a , b : ellipse semi-major axis, r_f : flow front radius, r_0 : injection radius, t : time, Δp : pressure difference between inlet and flow front.

K_e is then used to calculate K_1 and K_2 as follows:

$$K_1 = \frac{a}{b} K_e, K_2 = \frac{b}{a} K_e \tag{3}$$

When analyzing binder-free textiles the porosity can be calculated as:

$$\epsilon = 1 - V_f \tag{4}$$

For bindered textiles the porosity changes and is calculated by:

$$\epsilon = 1 - (V_f + V_b) \tag{5}$$

with V_b : binder volume fraction. Table 3 shows the increase in porosity according to Eq. 5 for the binder grammages used in this publication. It shows that even for small binder grammages the influence of the binder on the porosity is significant and should be considered when evaluating the results. However, the binder influence on porosity is often neglected in literature and permeability results of textiles with binder are presented based on fiber volume fraction only [5].

Table 2 Cavity heights and binder grammages

Cavity height	2,5 mm; V_f 40%	2,2 mm; V_f 45%	2 mm; V_f 50%	1,8 mm; V_f 55%
Binder grammage	20 g/m ²	0; 20 g/m ²	0; 20; 40; 80 g/m ²	0; 20 g/m ²

Table 3 Expected increase in preform porosity due to binder

Binder grammage	20 g/m ²	40 g/m ²	80 g/m ²
Expected increase in porosity according to Eq. 5	0.02	0.04	0.08

2.3 Binder Solubility and Influence on Cure

Binder-resin mixtures were heated to 22 °C, 40 °C, 80 and 120 °C and manually stirred to visually assess binder solubility at different temperatures. The temperatures were chosen to cover a wide range of possible process conditions. Room temperature is the recommended processing temperature of the resin, while 80 and 120 °C are included in different recommended curing cycles. 40 °C is the recommended working temperature of the binder. To further investigate the influence of binder on preform infusion and resin cure, separate binder-resin mixtures (5 g binder, 95 g resin) were magnetically stirred for 30 min at 40 °C, 80 and 120 °C. After cooling the mixtures back to room temperature 30 g of hardener was added and stirred into the mixtures for 2 min. Differential Scanning Calorimetry (DSC) and Rheometry samples were taken from the mixture and either immediately tested or stored at -20 °C to delay the cure reaction and tested within two days. If the binder did not fully dissolve in the resin, larger clumps of binder formed during mixing. These clumps were not included in the samples, thus altering the resin/binder ratio, which must be considered when evaluating the results. Binder-free samples were taken from a mixture of 100 g resin and 30 g hardener as a reference. Additional binder-resin mixtures (1 g binder, 19 g resin) were mixed to investigate the influence of binder on resin viscosity without hardener.

2.3.1 Differential Scanning Calorimetry (DSC)

DSC measurements were conducted to determine the influence of the binder on the glass transition temperature. The measurements were done on a TA Instruments Discovery DSC and analyzed using the associated TRIOS software. Three samples of 5–15 mg of each binder-resin-hardener mixture described in Sect. 2.3 were tested. Table 4 lists all samples tested. The test cycle consisted of an isothermal hold step at 80 °C for 120 min to fully cure the resin. The isothermal step was followed by a modulated temperature ramp (amplitude: 1.592 °C, period: 60 s) from -20 to 150 °C at a heating rate of 10 °C/min to determine the glass transition temperature of the cured mixtures.

2.3.2 Rheology

Table 4 provides an overview of all samples prepared for rheological testing. A TA Instruments Ares G2 Oscillation Rheometer was used for all measurements. The samples with hardener were cured at 40 and 80 °C to investigate the influence of the binder on the resin

Table 4 DSC and rheology sample preparation parameters. The DSC samples were mixed with hardener. The rheology samples were made with and without hardener

Samples	1	2	3	4
Stirred at (°C)	-	40	80	120
Binder added	No	Yes	Yes	Yes

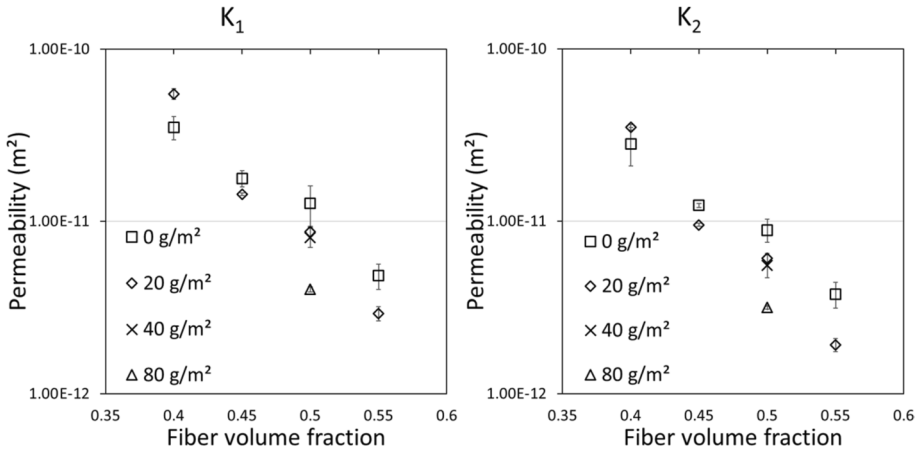


Fig. 6 Average permeability as a function of nominal fiber volume fraction for K_1 and K_2

cure by time sweeps. Parallel plates with a diameter of 25 mm were used. A gap of 0.5 mm was chosen, with an oscillation frequency of 1 Hz and a strain of 2%. The samples were placed in the rheometer at room temperature to avoid accelerating the cure process during the test preparation, especially for samples tested at 80 °C. Following the test preparation, the temperature was raised to the desired temperature using the rheometer's default heating rate (18 °C/min). Data recording began when the target temperature was reached. The samples were held at the target temperature until the measurement automatically stopped at a viscosity of approximately 10^6 Pa s.

In order to assess the influence of the binder on the viscosity of the resin, independent of the cure reaction, separate samples were prepared without hardener. Viscosity measurements were performed at four temperatures: room temperature (22 °C), 40 °C, 80 and 120 °C. Oscillatory tests were conducted with the specific parameters described above. Due to the high scatter of the results, the test method was modified to measure the viscosity rotationally at a frequency of 0.1 Hz. Larger parallel-plates with a diameter of 40 mm were used to improve the accuracy of measuring the low viscosities of the resin. The gap remained at 0.5 mm.

3 Results and Discussion

3.1 Permeability Measurement Results

The results of the permeability measurements were evaluated in two steps. First, the average permeability at each desired fiber volume fraction was calculated and analyzed. The permeability was then plotted as a function of the effective porosity. The results are shown in Figs. 6 and 8. Figure 6 shows mostly slightly lower permeability for the bindered textiles. Adding more binder to the preform (at 50% fiber volume fraction) reduces the permeability further. While the results for fiber volume fractions of 45%, 50%, and 55% follow the expected trend of decreasing permeability for increasing binder grammage due to additional volume added to the samples, the 40% samples show an increase in permeability after binder is added to the sample. This may be caused by inaccuracies in sample

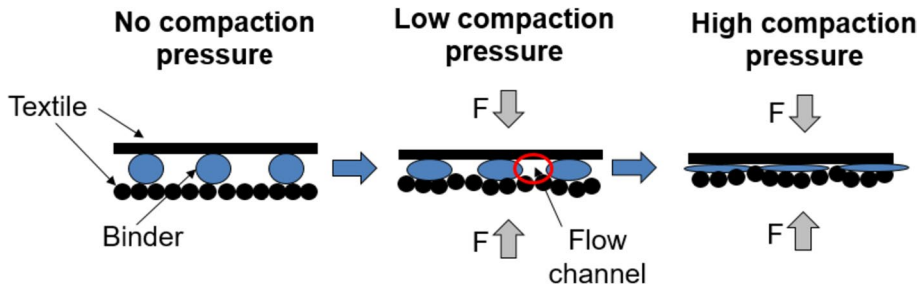


Fig. 7 Schematic drawing of the possible binder compaction during preforming at different compaction pressures

preparation or other variations within the fabric structure. While grammage variations are accounted for by weighing each layer before assembling the samples, other variations in the samples structure, such as loose sewing yarn, uneven binder spraying, small deviations in the orientation of the textile layers during stacking, or local fiber volume fraction variations cannot be detected by weighing. The samples were cut from two rolls of fabric of different production batches which may have been stored for different amounts of time before the samples were cut. However, during testing no indications for measurable differences between the textile rolls were found and the standard deviation for measurements of the same fiber volume fraction and binder grammage are small. The effect of local inhomogeneity within the samples is reduced by evaluating the permeability over a longer measuring distance. Another possible explanation for the higher permeability of the bindered samples at 40% fiber volume fraction can be found by looking at the behavior of long-chained powder binders during hot pressing, which has been studied in literature already. At elevated temperatures the viscosity of these powder binders is similar to the spray binder's viscosity at room temperature. Dickert [5] describes the behavior of a phenoxy-based powder binder (viscosity 8×10^5 Pa s) during hot pressing. The binder remains mostly between the fiber layers where it was applied. Due to its high viscosity it does not flow into the rovings despite capillary forces. However, with increasing compaction pressure, the binder particles start to deform into a flat shape ultimately leading to rearrangements in the fiber structure and changes in porosity as the binder is further pressed into the textile. At low compaction pressure the phenoxy binder is able to keep macro flow channels open and enhance resin flow as the compaction happens mostly within the fiber tows. This effect decreases with increasing compaction. At high compaction pressures the binder has lost its ability to enhance flow and instead obstructs resin flow and reduces the permeability. The spray binder may show similar behavior during preform compaction. At low compaction pressures, the binder may be able to enhance resin flow by delaying the closure of macro flow channels. At medium compaction pressures, the binder is then pressed flat and no longer supports the macro flow channels. Its effect on preform permeability changes from positive to neutral. At high compaction pressures, the binder is pressed further in between the fibers and begins to have a negative effect on preform permeability. Figure 7 shows a schematic drawing of the proposed binder behavior.

To further explore the compaction behavior of the spray binder the compaction pressure needed to reach fiber volume fractions of 40% and 45% were measured using the 20 N load cell of an Ares G2 rheometer for five round samples with a diameter of 26 mm and a binder grammage of 20 g/m². The samples were compacted with a punch-to-plate setup using a round punch with a diameter of 25 mm. A test speed of 1 mm/min was used. To reach a fiber volume

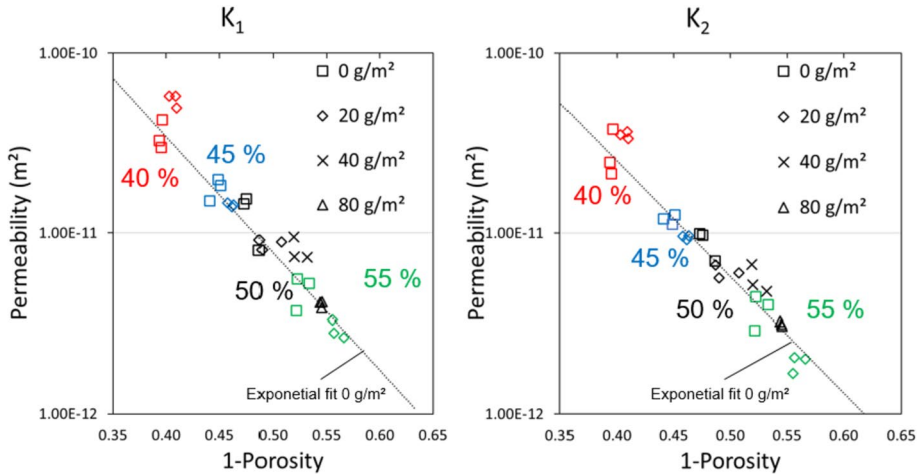


Fig. 8 Permeability as a function of 1-porosity for each individual measurement colored by nominal fiber volume fraction and exponential function for the 0 g/m² samples

fraction of 40% an average compaction force of 2.79 ± 0.37 N (equal to a pressure of 0.0057 N/mm²) was needed. For a fiber volume fraction of 45% the compaction force increased to 8.65 ± 0.95 N (equal to a pressure of 0.0176 N/mm²) which is roughly triple the compaction force for 40%. A fiber volume fraction of 50% could not be reached as compaction forces over 20 N are necessary. The binder is generally expected to increase the compaction pressure needed to reach a certain fiber volume fraction due to the restriction of the fibers degrees of freedom [5, 38]. For non-solid binder this effect is reduced and the compaction pressure needed to reach a desired fiber volume fraction is smaller than for solid binders [38, 39]. Wei et al. [40] report a high dependency of a liquid spray binder's resistance to deformation on the compaction speed due to creep and relaxation effects. At faster compaction speeds the binders resistance to deformation is increased. The spray binder used in this publication may be able to withstand the small compaction forces needed to reach 40% fiber volume fraction at the compaction speeds present in the permeability test rig. At higher fiber volume fractions the compaction forces increase rapidly and start deforming the binder into a flat shape.

Figure 8 shows the results of all permeability measurements at their respective porosities. The measured increase in porosity is close the expected values presented in Table 3. Compared to Fig. 6 this allows a comparison between the effects of the binder and an increase in fiber volume fraction as reasons for lower porosity. It also avoids biased results due to grammage variations between samples. The bindered samples tend to follow the exponential trend line of the results of the unbindered samples. This indicates that the spray binder has no additional effect on preform permeability other than increasing porosity (or the positive and negative effects cancel each other out). The 40% fiber volume fraction samples discussed previously still place above the unbindered samples when considering the measured porosity. The 45% and 50% bindered samples mostly follow the exponential trendline while the 55% samples place below the trend line. This finding further supports the theory presented above. However, to obtain definitive results a wider range of fiber volume fractions and binder grammages should be analyzed as the deviations from the unbindered trendline are small and may be the result of undetected variations in textile structure. Since the binder mostly increases the preform permeability similarly to an

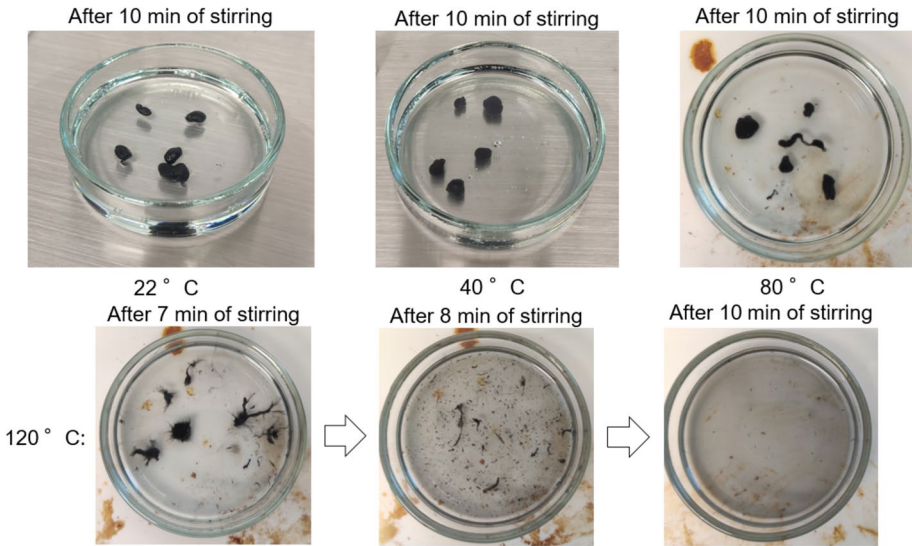


Fig. 9 Results of the solubility tests at different temperatures for binder (black) and resin (transparent)

increase in fiber volume fraction it is important to use the least amount of binder possible which still offers sufficient preform stability. The results further emphasize the complex relation between binder, textile and permeability as described in Sect. 1.

3.2 Binder Solubility

The results of the visual qualitative solubility testing are shown in Fig. 9. No interaction between binder and resin was observed for the mixtures stirred at 22 and 40 °C indicating no or minimal binder solubility when resin infusion is done at those temperatures. At 80 °C the binder viscosity is significantly reduced leading to deformations of the binder while stirring. However the binder is still visible as a separate phase after stirring and there is no visible dissolution. At 120 °C the binder viscosity is further reduced and the binder starts dissolving into the resin. The dissolution process is significantly faster when the mixture is stirred. Finally, the binder cannot visually be distinguished from the resin and only one grey liquid is visible. The binder stays dissolved in the resin after the mixture is cooled down to room temperature. During the different stages of liquid composite molding processes different temperatures are present. As the epoxy based spray binder is supposed to participate in the curing reaction with the hardener it is important to dissolve the binder in the resin at some point in the process chain. For the binder and resin system used in this article, the infused preform has to be heated to above 80 °C either during or after resin infusion. Before a final conclusion can be drawn on when to resolve the binder, the results of the DSC and rheology measurements have to be considered. They are presented and discussed in the following chapters.

3.3 Binder Influence on Glass Transition Temperature

The different glass transition temperatures T_g of the tested resin-binder-mixtures and different stirring temperatures are shown in Table 5. The results show glass transition

Table 5 Results of DSC measurements to determine binder influence on glass transition temperature

	Samples	Stirred at (°C)	T _g (°C)
No binder	1	-	85.7 ± 1.5
Binder	2	40	86.1 ± 4.0
	3	80	85.8 ± 1.6
	4	120	85.5 ± 0.5

temperatures around 86 °C for all tested samples regardless of binder content. Small differences between the samples are expected as the binder was added to the resin-hardener mixture as part of the resin. The ratio between resin and hardener changes when the binder does not dissolve or only partly dissolves within the resin (samples 2 and 3) from 100:30 to 95:30. All in all, the results indicate no influence of the binder on the glass transition temperature. This matches with results reported by Helber et al. [20] for different epoxy powder binders dissolved in epoxy resin. While the binder does not impact the glass transition temperature of the resin other curing characteristics of the mixture (e.g. total heat released or curing rate) may still be affected.

3.4 Binder Influence on Resin Cure Time and Viscosity

The results of the cure time measurements are shown in Fig. 10. The samples stirred at 120 °C seem to cure slightly faster than the samples where less/no binder was dissolved in the resin. The differences between the samples are small and may be caused by small differences in time from sample preparation to test start and slight changes in the mixing ratio of resin and hardener as described in Sect. 3.3. Determining the gel point was planned to further analyze the different curves. The gel point is the crossover of storage modulus G' and loss modulus G'' . However due to high scatter in the measurements of G' at low viscosities the gel point could not be determined using this method. Instead the time needed to reach a viscosity of 100 Pa s (criteria to determine dynamic gel point temperature during measurements with constant heating rate [19]) was compared between the samples. Table 6 contains the time needed to reach the target viscosity. Comparing the presented results with results reported in literature the differences between the samples are rather small. Brody and Gillespie [15] describe a doubling in curing time for a binder percentage of 5 wt% when using a thermoplastic binder in a thermoset matrix. Lionetto et al. [19] report a 50% decrease in curing time for samples where an epoxy binder (8.5 wt%) was dissolved in epoxy resin. Both used samples of similar weight than the samples prepared in this publication. The initial viscosities of the samples in this data set are not analyzed further. As described in Sect. 2.3.2 the oscillatory viscosity measurements did not lead to reproducible results at low viscosities below 1 Pa s. As a determination of the gel point as well as measuring the initial viscosity was not possible with the chosen test method the tests were stopped after one sample of each binder-resin mixture was tested at 40 and 80 °C.

The measured viscosities of the binder-resin mixtures without hardener are shown in Table 7. The mixture stirred at 120 °C where visible dissolution of the binder in the resin occurred has the highest viscosity at 22 and 40 °C. The viscosities of all other mixtures are almost identical at these temperatures. This is the expected result. Since there was no visible dissolution of the binder in the resin during stirring at 40 and 80 °C, the samples taken from these mixtures contain no or minimal amounts of binder. When the binder is

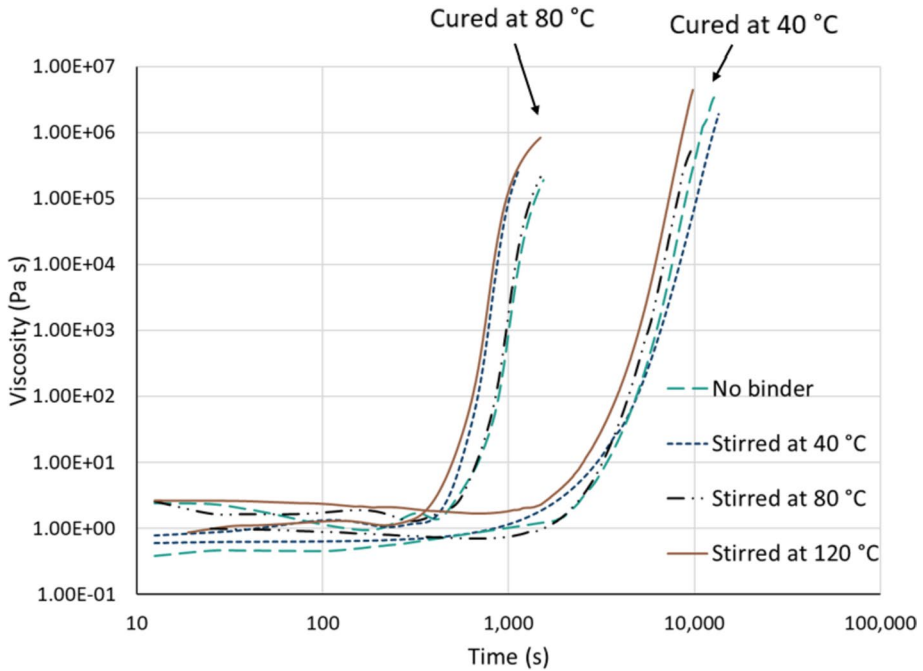


Fig. 10 Results of viscosity measurements to determine binder influence on cure time at 40 and 80 °C

fully dissolved in the resin, a higher viscosity is expected due to the higher initial viscosity of the binder. At high temperatures the highest viscosities were measured for the mixture stirred at 80 °C. However, since the standard deviation is almost as high as the measured values, the viscosities at 80 and 120 °C are not analyzed further.

Compared to powder binders the increase in viscosity when the binder is dissolved in resin is less. Dickert [5] reports a doubling of resin viscosity when 0.5 wt% of an epoxy powder binder are dissolved in epoxy resin and a tripling when the binder content is increased to 2 wt%. The samples prepared in this publication have binder contents of approximately 5 wt%. Powder binders have been measured to have viscosities in the range of 300 Pa s to 8×10^5 Pa s at their respective activation temperatures (90–160 °C) and are solid at room temperature [5]. The spray binder used in this publication has a viscosity of about 50 Pa s at 80 °C and about 3 Pa s at 120 °C [9, 41]. The reduced influence of the spray binder on resin viscosity may also lower the consequences of binder wash-out during resin infusion.

Table 6 Comparison of the time needed to reach a viscosity of 100 Pa s for each sample

	Cured at 40 °C	Cured at 80 °C
No binder	4876 s	884 s
Stirred at 40 °C	4907 s	670 s
Stirred at 80 °C	4450 s	854 s
Stirred at 120 °C	3820 s	639 s

Table 7 Viscosity of resin binder mixtures without hardener at different temperatures

	Viscosity at 22 °C	Viscosity at 40 °C	Viscosity at 80 °C	Viscosity at 120 °C
No binder	1.06 ± 0.020 Pa s	0.193 ± 0.015 Pa s	0.022 ± 0.016 Pa s	0.015 ± 0.011 Pa s
Stirred at 40 °C	1.03 ± 0.043 Pa s	0.184 ± 0.014 Pa s	0.023 ± 0.015 Pa s	0.017 ± 0.011 Pa s
Stirred at 80 °C	1.04 ± 0.047 Pa s	0.224 ± 0.013 Pa s	0.062 ± 0.014 Pa s	0.046 ± 0.016 Pa s
Stirred at 120 °C	1.59 ± 0.037 Pa s	0.405 ± 0.244 Pa s	0.041 ± 0.017 Pa s	0.016 ± 0.011 Pa s

3.5 Implications for Infusion Processes

The sample preparation techniques of the DSC and rheometer samples are not fully representative of real infusion processes. In real infusion processes, the binder is not dissolved in the resin at elevated temperatures, cooled down and then reheated. However, the results show the complex interaction between binder solubility and temperature, which must be evaluated for the specific binder-resin combination used in a particular manufacturing process. Three possible scenarios are discussed below. They are similar to scenarios discussed for powder binders by Dickert [5] and Tonejc [2]. However, the unique properties of the spray binder may open up new avenues for process design.

Scenario 1: Infusion and curing at low temperatures (< 40 °C)

The spray binder does not dissolve in the resin and reduces preform permeability during infusion. During resin cure, the binder may interact with the hardener. Depending on the spray pattern, uncured binder may remain in the final part and negatively affect its mechanical properties.

Scenario 2: Infusion at low temperatures (< 40 °C) and curing at high temperatures (> 100 °C)

The binder does not dissolve during resin infusion and reduces preform permeability. During resin cure, the binder dissolves in the resin if the curing time is sufficient. The binder participates in the curing reaction and no uncured binder should remain in the final part. The binder is uniformly distributed throughout the final part. No gradient in the mechanical properties is expected.

Scenario 3: Infusion and curing at high temperatures (> 100 °C)

The binder dissolves in the resin during infusion. This can lead to binder wash-out and binder accumulation at the flow front, ultimately resulting in higher resin viscosity and a slower infusion. In addition, a gradient in the mechanical properties could develop due to the uneven binder distribution within the final part. However, as shown in Sect. 3.4, the increase in resin viscosity due to dissolved binder is significantly less than for powder binder. Binder wash-out during resin infusion may be acceptable for spray binders. If the binder dissolves in the resin during infusion, the permeability of the preform may increase because the binder is no longer present in its highly viscous state obstructing resin flow.

When comparing the three scenarios, scenario 1 appears to be the most undesirable one. The binder does not fully dissolve in the resin and spots of uncured binder may remain in

the final part. Depending on the amount of binder used this could also change the stoichiometric ratio between resin and hardener. Scenario 2 is the “safest” way to produce a part with predictable binder distribution in the final part. The binder only dissolves in the resin during curing and the permeability of the preform remains constant throughout the infusion process. Scenario 3 may offer some potential for process adjustments if the resin system chosen for the infusion does not cure too quickly during infusion at high temperatures. As the binder dissolves during infusion the permeability of the preform may increase resulting in faster infusion. At the same time, the dissolved binder increases the viscosity of the resin thus increasing the infusion time. There may be a “sweet spot” where the resin infusion is faster than in scenario 2.

4 Conclusion

The influence of epoxy spray binder on preform permeability, glass transition temperature and resin cure time and resin viscosity was analyzed in this publication and compared to other binder types. The binder mainly lowers preform permeability especially when larger amounts of binder are applied to the textile and the fiber volume fraction is high. Therefore, it is important to evaluate the minimal amount of binder needed for sufficient preform fixation to reach the fastest process time and adjust the binder application process accordingly. At low fiber volume fractions the spray binder may have a positive effect on preform permeability and enhance resin flow. The influence of the binder on the infusion step is complex as further shown in the solubility, DSC and rheometer measurements. Depending on the temperatures present during the infusion process the binder may dissolve in the resin or remain as a separate phase. When dissolved the binder negatively influences the resin viscosity. Compared to powder binder and veils the effects on resin cure are less severe which make spray binders a good alternative for them. It is still important to study the interactions between the binder and the specific resin system used to avoid negative impact of the binder on the manufacturing process.

For a complete understanding the impact of epoxy spray binder on the mechanical properties has yet to be evaluated.

Acknowledgements The authors would like to thank the federal state of Lower Saxony and the European Regional Development Fund (ERDF) for financial and organizational support of the project AutoBLADE. The binder was supplied free of charge by CTP Advanced Materials.

Author Contributions All authors contributed to the study conception and design. Material preparation, data collection and analysis were performed by Hendrik Möllers. The first draft of the manuscript was written by Hendrik Möllers and all authors commented on previous versions of the manuscript. All authors read and approved the final manuscript.

Funding Open Access funding enabled and organized by Projekt DEAL.

Data Availability The data that support the findings of this study are available from the corresponding author upon reasonable request.

Open Access This article is licensed under a Creative Commons Attribution 4.0 International License, which permits use, sharing, adaptation, distribution and reproduction in any medium or format, as long as you give appropriate credit to the original author(s) and the source, provide a link to the Creative Commons licence, and indicate if changes were made. The images or other third party material in this article are included in the article’s Creative Commons licence, unless indicated otherwise in a credit line to the material. If material is not included in the article’s Creative Commons licence and your intended use is not

permitted by statutory regulation or exceeds the permitted use, you will need to obtain permission directly from the copyright holder. To view a copy of this licence, visit <http://creativecommons.org/licenses/by/4.0/>.

References

1. Cherif, C.: *Textile Werkstoffe für den Leichtbau*. Springer Berlin Heidelberg, Berlin, Heidelberg (2011)
2. Tonejc, M.: *Chancen und Herausforderungen bebindeter Textilien in der Faserkunststoffverbund-Verarbeitung*. Dissertation, Montanuniversität Leoben (2019)
3. Coutandin, S.: *Prozessstrategien für das automatisierte Preforming von bebinderten textilen Halbzeugen mit einem segmentierten Werkzeugsystem*. Dissertation, Karlsruher Institut für Technologie (2020)
4. Brody, J.C., Gillespie, J.W.: Reactive and non-reactive binders in glass/vinyl ester composites. *Polym. Compos.* **26**, 377–387 (2005). <https://doi.org/10.1002/pc.20068>
5. Dickert, M.: *Einfluss von Binder auf die Herstellung von Faserkunststoffverbunden*. Dissertation, Technischen Universität Clausthal (2015)
6. Ballier, F., Schwennen, J., Berkmann, J., et al.: The hybrid RTM process chain: Automated insertion of load introducing elements during Subpreform Assembling. *AMM* **794**, 312–319 (2015). <https://doi.org/10.4028/www.scientific.net/AMM.794.312>
7. Schmidt, S., Mahrholz, T., Kühn, A., et al.: Powder binders used for the manufacturing of wind turbine rotor blades. Part 1. Characterization of resin-binder interaction and preform properties. *Polym. Compos.* **39**, 708–717 (2018). <https://doi.org/10.1002/pc.23988>
8. Dickert, M., Ziegmann, G.: Influence of binder on the mechanical properties and the permeability of a non-crimp carbon fabric preform. *ECCM15–15th Eur. Conf. Compos. Mater.* (2012)
9. Möllers, H., Schmidt, C., Meiners, D.: Spray binder for automated preforming: Spray process and preform properties. *Polym. Compos.* (2022). <https://doi.org/10.1002/pc.27107>
10. Tanoglu, M., Robert, S., Heider, D., et al.: Effects of thermoplastic preforming binder on the properties of S2-glass fabric reinforced epoxy composites. *Int. J. Adhes. Adhes.* **21**, 187–195 (2001). [https://doi.org/10.1016/S0143-7496\(00\)00050-6](https://doi.org/10.1016/S0143-7496(00)00050-6)
11. Tanoğlu, M., Seyhan, A.T.: Investigating the effects of a polyester preforming binder on the mechanical and ballistic performance of E-glass fiber reinforced polyester composites. *Int. J. Adhes. Adhes.* **23**, 1–8 (2003). [https://doi.org/10.1016/S0143-7496\(02\)00061-1](https://doi.org/10.1016/S0143-7496(02)00061-1)
12. Helber, F., Carosella, S., Middendorf, P.: Quantitative assessment of reactive and non-reactive binder systems on first ply adhesion for dry fiber placement processes. *KEM* **926**, 1317–1326 (2022). <https://doi.org/10.4028/p-5j966g>
13. Coutandin S, Wurba A, Luft A et al (2019) Mechanical characterisation of the shear, bending and friction behaviour of bindered woven fabrics during the forming process. *Materialwiss Werkstofftech* **50**:1573–1587. <https://doi.org/10.1002/mawe.201900074>
14. Arnold, M., Stapf, D., Henne, M., et al.: Improvement of the toughness of epoxy resins systems using thermoplastic binders. In: *Sampe Europe 33rd International Conference and Forum* (2012)
15. Brody, J.C., Gillespie, J.W.: The effects of a Thermoplastic Polyester Preform Binder on Vinyl Ester Resin. *J. Thermoplast. Compos. Mater.* **18**, 157–179 (2005). <https://doi.org/10.1177/0892705705043535>
16. Bulat, M., Heieck, F.: *Binder Application Methods for Textile Preforming Processes*. Luftfahrttechnisches Handbuch (2015)
17. Girdauskaite, L., Krzywinski, S., Rödel, H., et al.: Local structure fixation in the Composite Manufacturing Chain. *Appl. Compos. Mater.* **17**, 597–608 (2010). <https://doi.org/10.1007/s10443-010-9130-6>
18. Tanoğlu, M., Seyhan, A.T.: Compressive mechanical behaviour of E-glass/polyester composite laminates tailored with a thermoplastic preforming binder. *Mater. Sci. Eng. A* **363**, 335–344 (2003). <https://doi.org/10.1016/j.msea.2003.08.005>
19. Lionetto, F., Moscatello, A., Maffezzoli, A.: Effect of binder powders added to carbon fiber reinforcements on the chemoreology of an epoxy resin for composites. *Compos. Part B: Eng.* **112**, 243–250 (2017). <https://doi.org/10.1016/j.compositesb.2016.12.031>
20. Helber, F., Szesny, M., Carosella, S., et al.: Enhancement on automated preforming for composite structures. *ICCM* **22** (2019)
21. Becker, D., Mitschang, P.: Influence of preforming technology on the out-of-plane impregnation behavior of textiles. *Compos. Part A: Appl. Sci. Manuf.* **77**, 248–256 (2015). <https://doi.org/10.1016/j.compositesa.2015.05.001>
22. Estrada, G., Vieux-Pernon, C., Advani, S.G.: Experimental characterization of the influence of Tackifier Material on Preform Permeability. *J. Compos. Mater.* **36**, 2297–2310 (2002). <https://doi.org/10.1177/0021998302036019542>

23. Magagnato, D., Thoma, B., Henning, F.: Experimental characterization to determine the influence of different binder systems on the preform permeability during RTM manufacturing. *Z. Kunststofftechnik* **1**, 256–270 (2015). <https://doi.org/10.3139/O999.03042015>
24. Yoo, H.M., Lee, J.W., Kim, J.S., et al.: Influence of non-reactive Epoxy Binder on the permeability and friction coefficient of Twill-Woven Carbon Fabric in the Liquid Composite Molding process. *Appl. Sci.* **10** (2020)
25. Grou, L., Hubert, P.: Experimental permeability evaluation of banded preform. In: *The 14th International Conference on Flow Processes in Composite Materials* (2018)
26. Shih, C.-H., Lee, L.J.: Tackification of Textile Fiber preforms in Resin transfer molding. *J. Compos. Mater.* **35**, 1954–1981 (2001). <https://doi.org/10.1106/Y1JX-HB8L-9DX5-YJK1>
27. George, A.: Optimization of resin infusion processing for composite materials. Dissertation, Universität Stuttgart (2011)
28. Denkena, B., Schmidt, C., Werner, S., et al.: Development of a shape replicating draping unit for continuous layup of unidirectional Non-crimp fabrics on Complex Surface geometries. *J. Compos. Sci.* **5** (2021). <https://doi.org/10.3390/jcs5040093>
29. Bogenschütz, M., Möllers, H., Stüven, J.-L., et al.: Automatisierte Preform-Fertigung. *VDI-Z* **165**, 51–53 (2023). <https://doi.org/10.37544/0042-1766-2023-05-51>
30. Abliz, D., Berg, D.C., Ziegmann, G., et al.: In-plane and Out-of-plane Permeability Characterization of Technical Textiles. Tagungsband 3. Symposium Materialtechnik (2019)
31. Abliz, D.: Functionalization of fiber composites with nanoparticle-modified resin systems. Dissertation, Technische Universität Clausthal; Papierflieger Verlag (2017)
32. Fauster, E., Berg, D.C., Abliz, D., et al.: Image processing and data evaluation algorithms for reproducible optical in-plane permeability characterization by radial flow experiments. *J. Compos. Mater.* **53**, 45–63 (2019). <https://doi.org/10.1177/0021998318780209>
33. Arbter, R., Beraud, J.M., Binetruy, C., et al.: Experimental determination of the permeability of textiles: A benchmark exercise. *Compos. Part A: Appl. Sci. Manuf.* **42**, 1157–1168 (2011). <https://doi.org/10.1016/j.compositesa.2011.04.021>
34. May, D., Aktas, A., Advani, S.G., et al.: In-plane permeability characterization of engineering textiles based on radial flow experiments: A benchmark exercise. *Compos. Part A: Appl. Sci. Manuf.* **121**, 100–114 (2019). <https://doi.org/10.1016/j.compositesa.2019.03.006>
35. Vernet, N., Ruiz, E., Advani, S., et al.: Experimental determination of the permeability of engineering textiles: Benchmark II. *Compos. Part A: Appl. Sci. Manuf.* **61**, 172–184 (2014). <https://doi.org/10.1016/j.compositesa.2014.02.010>
36. Yong, A., Aktas, A., May, D., et al.: Out-of-plane permeability measurement for reinforcement textiles: A benchmark exercise. *Compos. Part A: Appl. Sci. Manuf.* **148** (2021)
37. Darcy, H.: *Les Fontaines Publiques de la ville de Dijon: Exposition et Application Des Principes à Suivre et des formules à Employer dans les questions de distribution d'eau ...* V, Dalmont, Paris (1856)
38. Wu, W., Jiang, B., Xie, L., et al.: Effect of Compaction and Preforming parameters on the Compaction Behavior of Banded Textile Preforms for Automated Composite Manufacturing. *Appl. Compos. Mater.* **20**, 907–926 (2012). <https://doi.org/10.1007/s10443-012-9308-1>
39. Mei, M., Sun, L., Yujia, H., et al.: Preforming characteristics in compaction process for fabric with binder under elevated temperature. *Compos. Commun.* **23** (2021)
40. Wei, K., Liang, D., Mei, M., et al.: Preforming behaviors of carbon fiber fabrics with different contents of binder and under various process parameters. *Compos. Part B* **166**, 221–232 (2019). <https://doi.org/10.1016/j.compositesb.2018.11.143>
41. CTP Advanced Materials GmbH: TDS CeTePox AM 1010. Preliminary technical data sheet (2020)

Publisher's Note Springer Nature remains neutral with regard to jurisdictional claims in published maps and institutional affiliations.